JOURNAL OF MATERIALS SCIENCE **36** (2001) 1995–2000

Effect of heating temperature on dielectric properties of $Pb(Zr,Ti)O_3$ [PZT] fibers

YONG-IL PARK*
Advanced Research Center for Energy and Environment, Musashi Institute of Technology, 1-28-1 Tamazutsumi, Setagaya-ku, Tokyo 158-8557, Japan
Department of Applied Chemistry, Graduate School of Engineering, the University of Tokyo, 4-6-1 hongo, Bunkyo-ku, Tokyo 113-8656, Japan
E-mail: park@imat.chem.t.u-tokyo.ac.jp

MASAYUKI NAGAI
Advanced Research Center for Energy and Environment, Musashi Institute of Technology, 1-28-1 Tamazutsumi, Setagaya-ku, Tokyo 158-8557, Japan

MASARU MIYAYAMA, TETSUICHI KUDO
Department of Applied Chemistry, Graduate School of Engineering, the University of Tokyo, 4-6-1 hongo, Bunkyo-ku, Tokyo 113-8656, Japan

Ferroelectric $Pb(Zr_{0.53}Ti_{0.47})O_3$ fibers were reproducibly fabricated by sol-gel technique using triethanolamine (TEA) complexed alkoxide. The phase transition from pyrochlore to perovskite took place about 400°C and a stable single perovskite phase was obtained at 550°C. PZT gel fibers spun through nozzle were heat-treated at 700°C, and at 1000°C for 1 h to certify the effect of heat-treatment temperature on the electrical properties. The PZT fibers had elliptical cross sections with diameter of 72 μm–92 μm, and dense microstructure was obtained by heating at 1000°C. In the PZT fibers heat-treated at 1000°C, a distinguishable relative permittivity peak and a pyroelectric current peak were observed at their Curie temperature. The P-E hysteresis loops of the crystalline PZT fibers were also observed.

1. Introduction

PZT($Pb(Zr,Ti)O_3$) has been reported that has perovskite structure, high curie point and spontaneous polarization. For its ferroelectric and pyro-piezoelectric properties, many reports on the sol-gel derived PZT powders and thin films have been published, but few reports on the fibrous one. A fibrous form is preferred geometry for the reduction of heat capacity and the increase of responsivity in small scale devices. Generally speaking, fiberization of the functional ceramics, not necessarily to PZT, will expand their utility in the micro device such as sensors. However, conventional melt-processing routes to fibers cannot be used because of incongruent melting and volatility of Pb at high temperature. Therefore, some kinds of ferroelectric oxide fibers have been prepared from metal alkoxide solutions by sol-gel processing, namely $LiNbO_3$ [1], $BaTiO_3$ [2], $PbTiO_3$ [3–6], PZT [7, 8] and PLZT [9] fibers. These fibers are attractive for many applications, such as sensors, hydrophones and transducers [9, 10]. However, most of studies on these functional fibers have been limited to only the processing procedures because of the difficulty in fabrication of crack-free fibers, and in electrical characterization due to their extremely small electrical output signal.

A series of successful routes for sol-gel derived fiber fabrication using the nitrogen-doner stabilization agent, as like ethylenediamine [11], isopropylamine [12] and alkanolamine [13] to control hydrolysis reaction of metal alkoxides have been proposed. Especially for titanium alkoxide, β-diketone and alkanolamine have been generally used to control rapid hydrolysis reaction because the electronegativity of Ti atom is low and the partial charge of Ti atom is large ($\delta_{(Ti)} = +0.60$). It has been reported in past papers [14, 15] that triethanolamine (TEA) has two important effects; (1) The addition of TEA to the alcoholic solutions of alkoxides suppress their hydrolysis giving homogeneous, stable sols without the occurrence of gel formation or precipitation. (2) The presence of TEA enhances the solubility of the alkoxides and metallic salts such as lead acetate trihydrate into alcoholic solutions. Details of the effect of TEA on the $PbTiO_3$ or PZT solution synthesis procedure are reported elsewhere [6, 8].

In this paper, we investigated the electrical properties including ferroelectric and pyroelectric properties of PZT fibers derived from TEA-stabilized sol, and the heat-treatment temperature effect on their electrical properties.

* Author to whom all correspondence should be addressed.

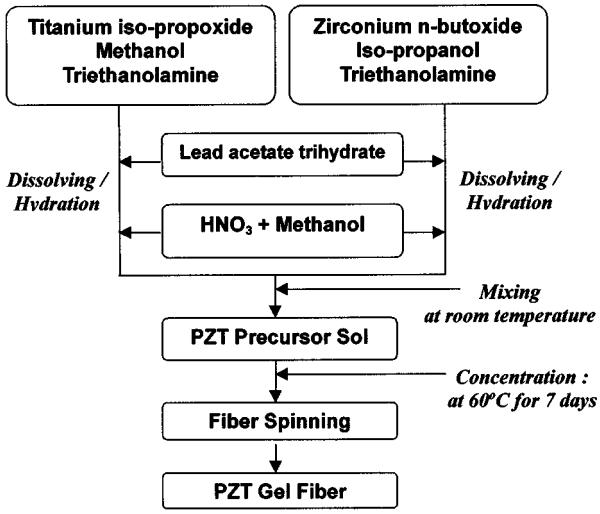

Figure 1 Flow diagram for PZT fiber processing.

2. Experimental procedure

2.1. Sample preparation and characterization

The procedure for producing $Pb(Zr_{0.53}Ti_{0.47})O_3$ [PZT] fibers in this study is briefly illustrated in Fig. 1. Methanol was used as an alcoholic medium in this sol-gel processing. In the present procedure, the PZT precursor solution was prepared simply by mixing lead acetate trihydrate [$Pb(CH_3COO)_2 \cdot 3H_2O$], triethanolamine [TEA, $N(C_2H_5OH)_3$], titanium isopropoxide [$Ti(OPr^i)_4$] and zirconium normal butoxide [$Zr(OBu^n)_4$] at room temperature. HNO_3 was added to the precursor solution to ensure condensation and hydrolysis reaction.

The obtained solution was concentrated in a bottle (1.5 cm in diameter and 5 cm in height) capped with five holes (0.5 mm in diameter) at 60°C for 7 days so as to reach to a spinnable viscosity. The spinnability was empirically examined by drawing method with a glass rod. The gel fibers were obtained by extrusion the concentrated precursor solution through a spinneret with one 200 μm diameter hole at a pressure of 1 Mpa. Then the fibers were dried for 2 days at room temperature and 3 days at 120°C. Obtained gel fibers were cut by 2 cm long and set on platinum substrate for heat-treatment. To certify the effect of firing temperature, two samples were prepared as shown in Table I. Sample A was heat-treated at 700°C for 1 hr in air, and sample B was at 1000°C for 1 h in Pb atmosphere. The fibers were heated up at a rate of +0.5°C/min to 600°C, and then at +5°C/min over 600°C. Phase analysis for the fibers were performed using X-ray diffraction (XRD) analysis. A field emission scanning electron micrograph (FE-SEM) was used for microstructural analysis.

TABLE I Samples prepared for this study

Sample	Heat treatment temperature (°C)	Keeping time (h)	Atmosphere	Composition
A	700	1	in air	PZT(53/47)
B	1000	1	in Pb	

2.2. Electrical measurements

The frequency dependence of permittivity and dissipation factor at room temperature were obtained using an impedance analyzer (YHP 4194A) at a frequency in the range of 1 kHz to 40 MHz. For the extremely small output signals (capacitance less than 1 fF for each fiber), bundles of thirty fibers cut by 3 mm long were used in order to amplify the electric signals for electrical characterization in this work. A silver paste (Screen Print 7095, Dupont) was painted to both ends of the fibers and then heat-treated at 450°C to set them and ensure electrical contact. Areas of fiber cross sections were confirmed through direct SEM observations. The relative permittivity change with temperature of the fibers was obtained using precision LCR meter (YHP 4284A). The heating rate was +3°C/min. P-E hysteresis loops of the fibers were obtained using RT6000HVS in silicon oil bath at room temperature. Pyroelectric current was measured using a picoammeter (YHP 4140B pA meter) connected to the electrodes, while the sample was heated up rapidly at a heating rate of +13°C/min from room temperature to 540°C. Before the measurement, the sample was poled at 150°C in silicon oil bath with dc electric field of 20 kV/cm.

3. Results and discussion

3.1. Sol-gel transition and thermal evolution

Fig. 2 shows FT-IR spectrum of the PZT gel powders prepared by drying the precursor solution. An intense peak ascribable to acetyl group was observed at 1410 cm^{-1}. The band around 3400 cm^{-1} and a shoulder around 1700 cm^{-1} are due to the absorbed water. The peak at 1570 cm^{-1} is assignable to the shifted peak of lead acetate trihydrate at 1550 cm^{-1}. This shifting has been reported as an indication of the formation of Ti-O-Pb(OAc) chain [4],

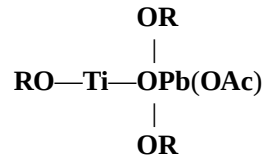

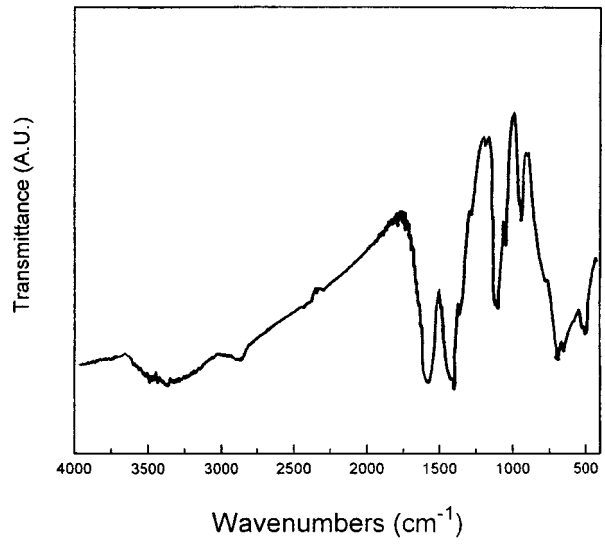

Figure 2 FT-IR spectrum of the dried PZT gel powders.

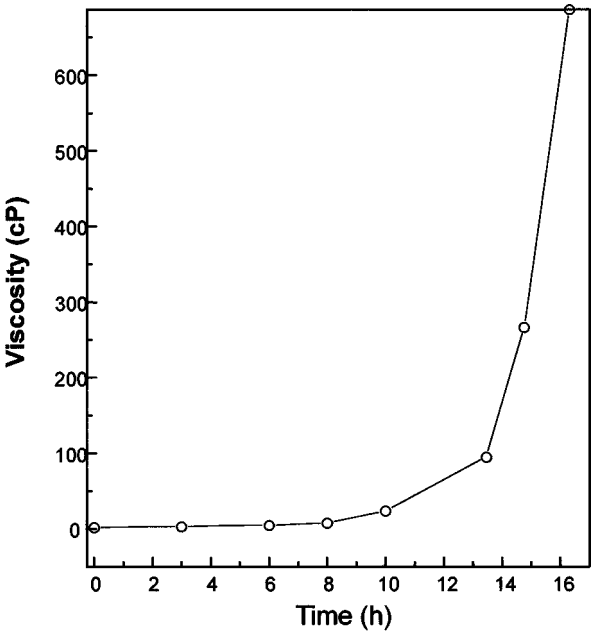

Figure 3 Viscosity change of PZT sol at 60°C as a function of time.

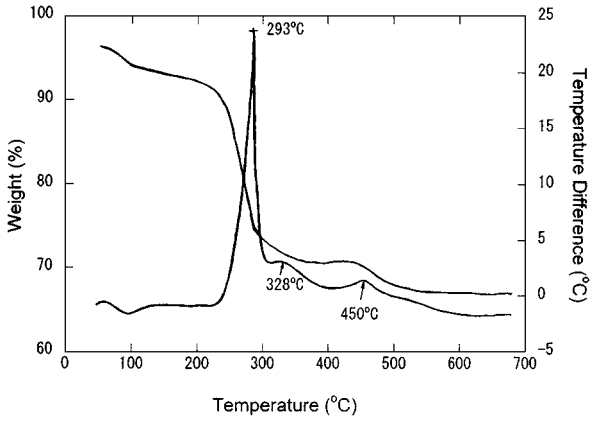

Figure 4 DTA-TG curves for the dried gel fibers.

where R denotes alkyl group and Pb(OAc) denotes lead acetate, $Pb(OCH_3COO)$.

A small peak around 1100 cm^{-1} shows N-C bond of TEA, and the band over the low wavenumber range (500–700 cm^{-1}) is assignable to formation of Ti-O bonds from the accelerated polycondensation reaction promoted by acidic catalyst in sol-gel transition state. Viscosity change of PZT sol at 80°C as a function of time is shown in Fig. 3. At first state (0–10 h), almost no difference was observed. After 14 h, the viscosity of the samples drastically increased and reached to spinnable viscosity as concentration and volatilization of solvent proceeds. Fibers were successfully drawn when the solution viscosity reached to about 10^4 cp.

DTA-TG curves for the dried gel fibers are shown in Fig. 4. Small endothermic peaks observed at 60°C–110°C are attributed to evaporation of absorbed water and alcohol. Large weight loss of about 20% accompanying a sharp exothermic peak around 290°C should be due to the drastic removal of acetyl groups and bonded alkyl groups. Some combustion loss (about 10%) accompanying small exothermic peak around 450°C seems to be due to the combustion of TEA.

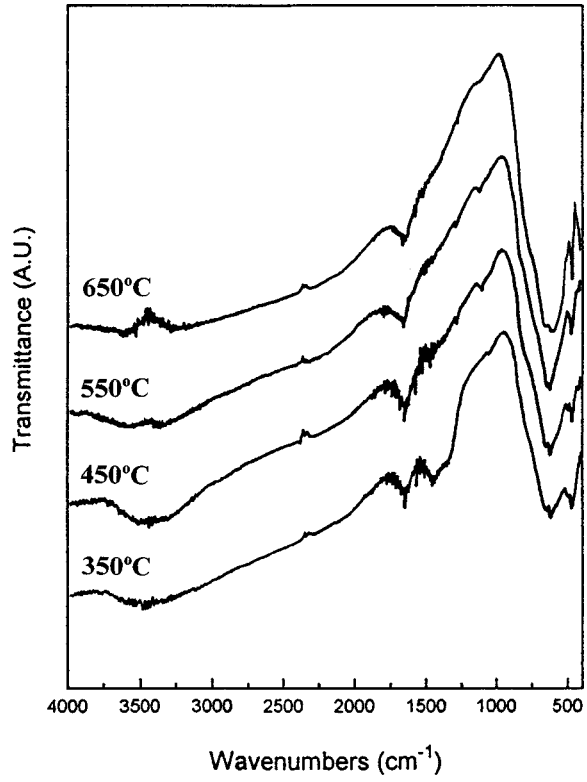

Figure 5 FT-IR spectra of the PZT gel powders at different heat-temperature.

Fig. 5 shows FT-IR spectra of the PZT gel powders at different heat-temperature. A peak around 1410 cm^{-1} by acetyl group is weaken as temperature goes up, and then disappeared at 550°C. The N-C bond by TEA-alkoxide reaction at 1100 cm^{-1} is found even at 550°C indicating the combustion of TEA compounds continues after pyrochlore-perovskite phase transition at 450°C. The X-ray diffraction (XRD) patterns of the PZT gel powders at different heat-treatment temperature are shown in Fig. 6. Pyrochlore phase at 350°C, and a mixed phase of pyrochlore and perovskite were observed at 450°C. As heating temperature increased to 550°C, the pyrochlore phase disappeared and transited to single perovskite phase.

3.2. Shapes and microstructures

Fig. 7(a) shows the fractured cross section of a PZT gel fiber dried at 120°C for 3 days. The cross sections of gel fibers have elliptical shapes. It has been reported that the shape of nozzle and the viscosity of the concentrated solution have no effect on the cross-sectional shape of the fiber, the only factor that affects its shape is the shrinking ratio of the gel fiber during spinning [16]. Therefore, the elliptical shape of cross section of the PZT fibers is assignable to large organic content including TEA in the precursor solution. The average diameter of the gel fibers was 136 μm and their surfaces were very smooth due to their high organic content. After heat-treatment procedure, the fibers show crystalline surfaces and cross sections ((b)–(d) in Fig. 7). The average diameters of the fabricated PZT fibers were 92 μm for sample A (heat-treated at 700°C for 1 h, in air), and 72 μm for sample B (heat-treated at 1000°C for 1 h, in Pb atmosphere). The calculated shrinkage ratios

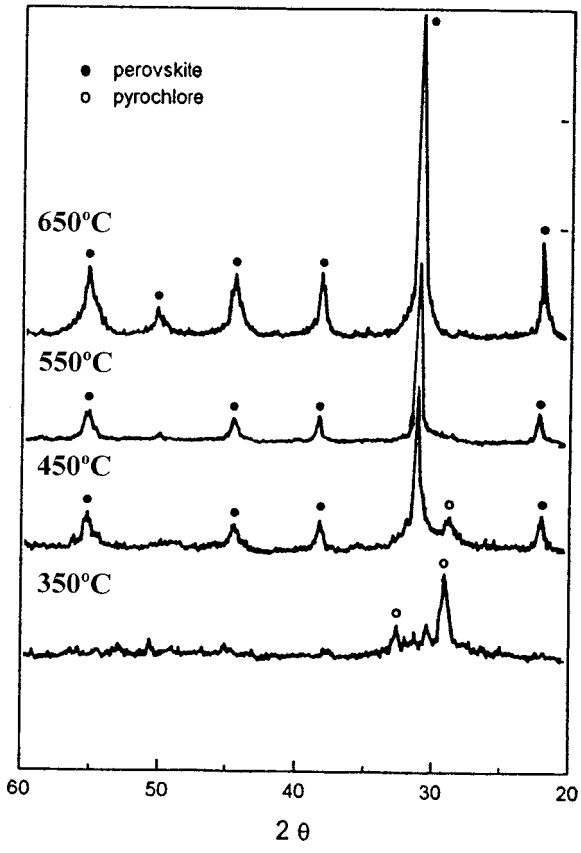

Figure 6 XRD patterns of the PZT gel powders at different heat-treatment temperature.

to the average diameter of dried gel fibers were 33% and 48% for sample A and B, respectively. Therefore, condensation of PZT fibers is found to continue in the temperature range of 700°C–1000°C. The microstructures of the sample A and B are shown in Fig. 7(e) and (f) respectively. The average grain size drastically increased from 0.2 μm of sample A to 0.8 μm of sample B. Many pores which is observed in interior of sample A significantly decreased in sample B.

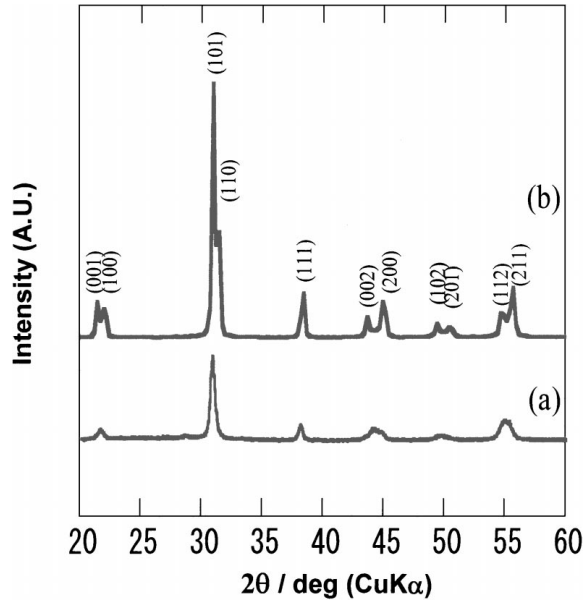

Figure 8 XRD plots of PZT fibers; (a) Sample A (sintered at 700°C for 1 h, in air), (b) Sample B (sintered at 1000°C for 1 h, in Pb atm).

XRD patterns for sample A and B are illustrated in Fig. 8. Both samples showed perovskite single phase, and relatively improved crystallinity was observed in sample B compared to that of sample A. Crystal orientation could not be found in both samples in spite of the high possibility of crystal orientation due to stress gradient which might be formed during fiber spinning.

3.3. Electrical properties

Fig. 9 shows the relative permittivity and tan δ of the fibers as a function of frequency at room temperature. The measured relative permittivity shows remarkable dependence upon heat-treatment temperature. The permittivity of sample A is much lower than that of sample B. From the porosity dependence of permittivity

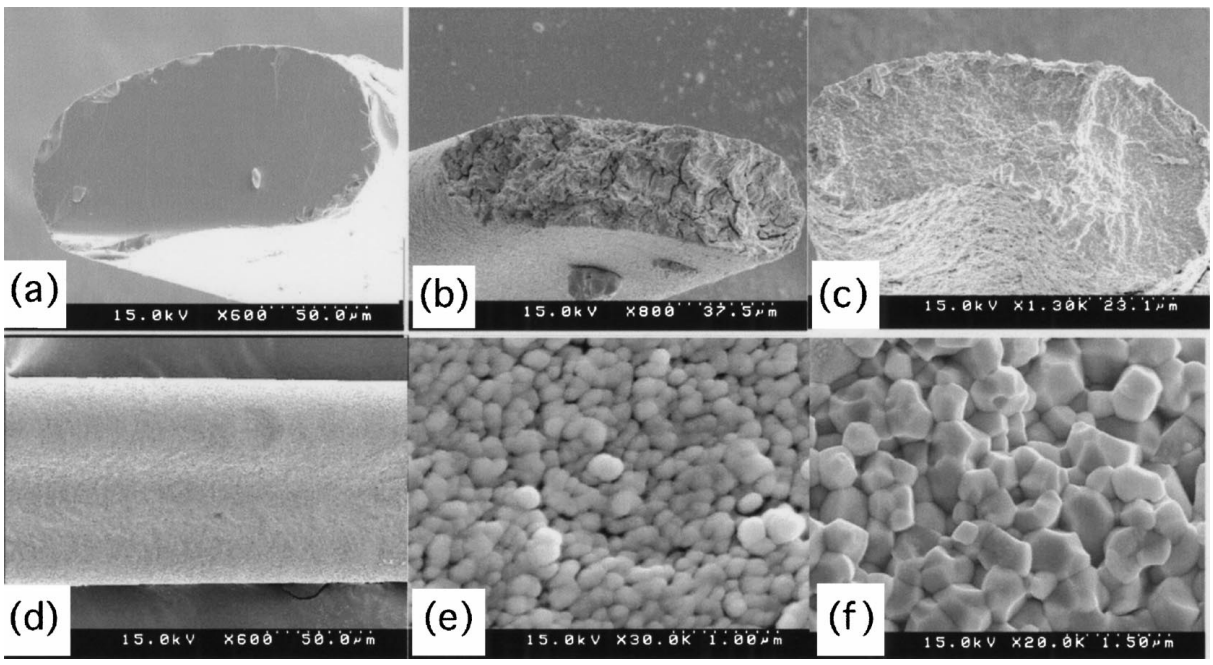

Figure 7 SEM micrographs of PZT fibers; the cross sections and surface of fibers (a) dried at 120°C, (b) sintered at 700°C, (c) and (d) sintered at 1000°C; and the microstructures of fibers (e) sintered at 700°C and (f) 1000°C.

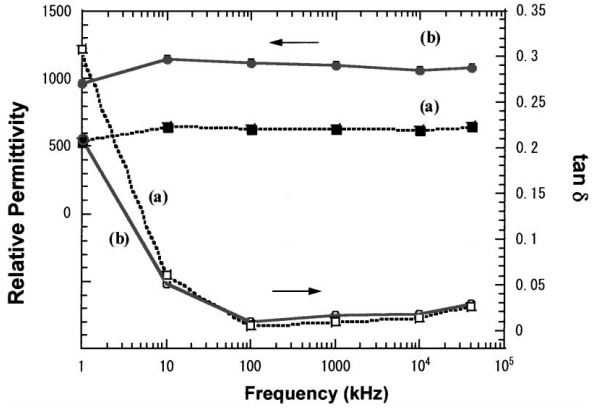

Figure 9 The relative permittivity and loss tangent changes of PZT fibers as a function of frequency at R.T.; (a) Sample A (sintered at 700°C for 1 h, in air) (b) Sample B (sintered at 1000°C for 1 h, in Pb atm).

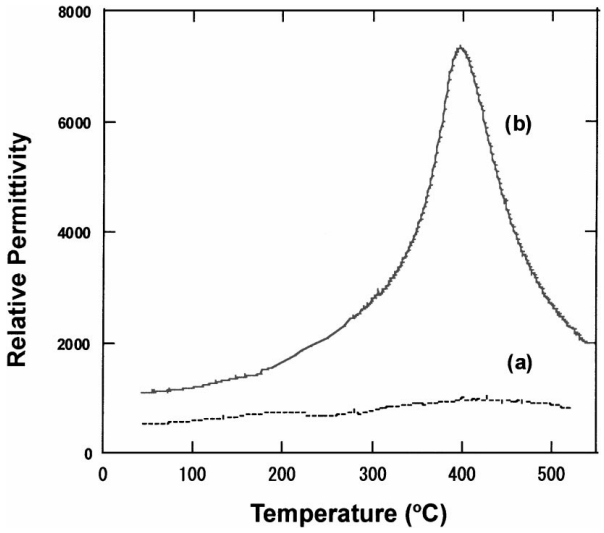

Figure 10 Relative permittivity as a function of temperature for PZT fibers, (a) Sample A (sintered at 700°C for 1 h, in air), (b) Sample B (sintered at 1000°C for 1 h, in Pb atm).

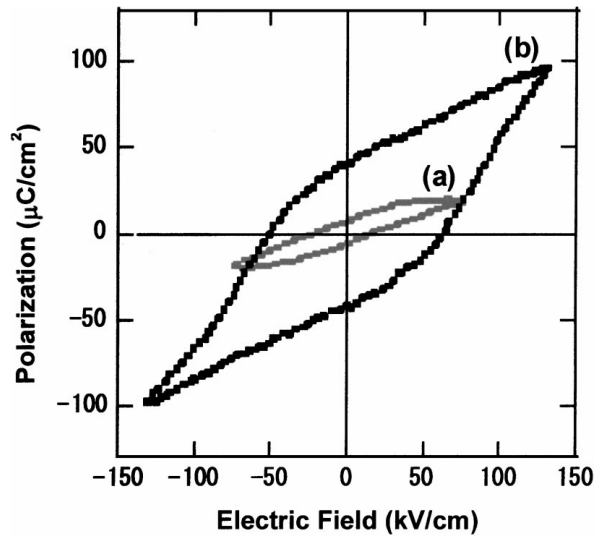

Figure 11 Hysteresis loops of PZT fibers; (a) Sample A (sintered at 700°C for 1 h, in air), (b) Sample B (sintered at 1000°C for 1 h, in Pb atm).

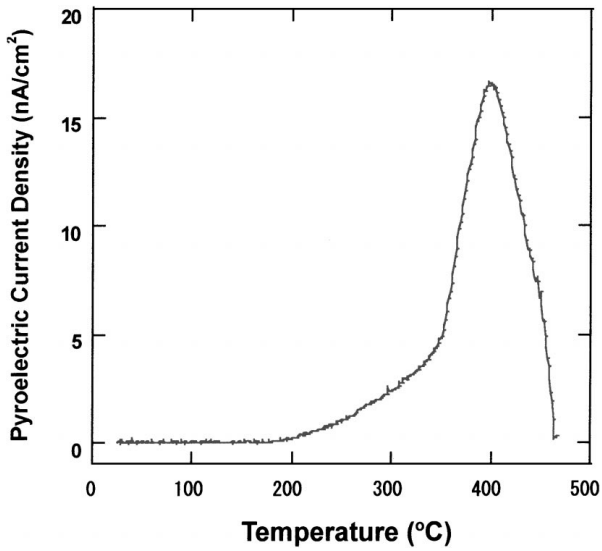

Figure 12 Pyroelectric current density of PZT fibers (Sample B (sintered at 1000°C for 1 h, in Pb atm)).

reported before [17, 18], the reasons of the low permittivity of sample A should be; (1) a decreased dipole moment efficiency at unit volume due to relatively small grain size, (2) an increased depolarizing field due to relatively low density and large porosity from small concentration rate (33%). Sample A showed larger tan δ than those of sample B in low frequency region implying occurring of space charge polarization due to high porosity. Fig. 10 shows relative permittivity as a function of temperature for (a) sample A and (b) sample B. A sharp permittivity peak was observed in sample B at 396°C which is vicinity of the reported T_c of PZT(53/47) ceramics, while sample A showed low permittivity values and an broad peak.

Ferroelectric hysteresis loops for sample A and B were observed in the range of electric field of $\sim\pm$ 140 kV/cm as shown in Fig. 11. A typical ferroelectric hysteresis loop was observed in sample B, while electrical breakdown occurred around $\pm$80 kV/cm in sample A. The remnant polarization, $+P_r$, of 41 μC/cm^2 and the coercive field $+E_c$ of 61 kV/cm were obtained in sample B. In spite of large applied electric field which is enough to obtain saturated polarization state in PZT bulk ceramics, saturated hysteresis loop could not be obtained and the Pr values was too high in the fibers. This may be due to; (1) high organic content that remained in fibers by insufficient burnout. Large amount of TEA (b.p. = 271°C) used for stabilization of solution may cause the large leakage current density resulting larger P_r value than bulk ceramics. (2) non-switching linear response due to space charge polarization [19] that is originated from pores reside in porous microstructure due to high organic content of starting solutions.

For the poled sample B ($E_p = 20$ kV/cm, at 150°C for 2 h), a large pyroelectric current was observed (Fig. 12). Pyroelectric current of sample A could not characterized because electrical breakdown occurred during poling procedure. The range of temperature in which pyroelectric current was detected was 25°C–460°C. A distinguishable pyroelectric current peak that have been reported in many ferroelectric bulk ceramics, $BaTiO_3$ [20], PZT [21], $Sr_{1-x}Ba_xNb_2O_6$ [22, 23], was also observed in this study. The pyroelectric current peak is located at 398°C, that is almost same

temperature with the permittivity peak as shown in Fig. 10. There were three steps in increasing rate of pyroelectric current. Very small pyroelectric current was detected until temperature reached to 172°C (region I in Fig. 12). In region II, 170°C–350°C, there was a slow increase in pyroelectric current, and then a drastic jump in region III, 350°C–398°C. As heating up above 398°C the current started to drop, and disappeared around 460°C by depolarization.

Pyroelectric coefficient was derived from the measured current density through following equations [22, 23];

$$i_p = (dP_s/dT) \cdot (dT/dt)$$

$$p = |(dP_s/dT)| \, [C \cdot cm^{-2} \cdot K^{-1}]$$

where,

i_p: pyroelectric current density
P_s: spontaneous polarization
T: temperature
t: time
p: pyroelectric coefficient.

The calculated pyroelectric coefficient, p, of sample B was very large (76.5 nC/cm^2 K) around 398°C. The microstructural benefits of sample B discussed in previous section may be the reason of distinguishable improvement in ferroelectric and pyroelectric properties [24].

Obtained electrical properties of PZT fibers are listed in Table II. From above results, it can be said that the heat-treatment temperature for PZT fibers should be carefully chosen for actual ferroelectric or pyroelectric applications.

4. Summary

The Pb(Zr,Ti)O_3 [PZT] precursor solutions were prepared from TEA-modified metal alkoxides, and the gel fibers were formed by extrusion viscous solution.

The average diameter of the heat-treated PZT fibers was 72 μm–92 μm. The phase transition from pyrochlore to perovskite took place about 400°C and stable single perovskite phase was obtained at 550°C.

It was confirmed that the PZT fibers heat-treated 700°C or 1000°C have ferroelectric property. The relative permittivity of the fibers heat-treated at 700°C is much lower than those of the fibers heat-treated at 1000°C. In the fibers heat-treated at 1000°C, evident pyroelectric peak was observed at vicinity of the curie temperature. P-E hysteresis loops of the fibers were also observed in both samples sintered at 700°C and 1000°C, but the sample heat-treated at 700°C showed electrical breakdown at low electric field. The fibers heat-treated at 1000°C showed square-shaped hysteresis loop and large P_r and E_c. A large pyroelectric current was also observed in the fibers heat-treated at 1000°C, the measured pyroelectric coefficient p (nC $\cdot$ cm^{-2} $\cdot$ K^{-1}) increased up to 76.5 around 398°C. The increased electrical properties of the fibers heat-treated at 1000°C compared to those heat-treated at 700°C is attributed to the large grain size and decreased porosity.

TABLE II Electrical properties of $Pb(Zr_{0.53}Ti_{0.47})O_3$ fibers at room temperature

Properties	Sample A (700°C/1h, in air)	Sample B (1000°C/1h, in Pb atm.)
Average diameter (μm)	92	72
Average grain size (μm)	0.22	1.34
Relative permittivity $\varepsilon/\varepsilon_0$ (at 1 MHz)	633	1097
Tan δ (at 1 MHz)	0.001	0.015
Remnant polarization P_r (μC/cm^2)	—	41
Coercive field E_c (kV/cm)	—	61
Breakdown Strength E_b (kV/cm)	80	160
Pyroelectric coefficient p(nC/cm^{2}K, 25°C∼398°C)	—	25°C–170°C : ∼0.1 170°C–350°C : 0.1–21.5 350°C–398°C : 21.5–76.5

References

1. S. HIRANO, T. HAYASHI, K. NOSAKI and K. KATO, *J. Am. Ceram. Soc.* **72** (1989) 707.
2. T. YOKO, K. KAMIYA and K. TANAKA, *J. Mater. Sci.* **25** (1990) 3922.
3. S. I. AOKI, S. C. CHOI, D. A. PAYNE and H. YANAGIDA, "Better Ceramics through Chemistry IV" (Material Research Society, Pennsylvania, 1990) p. 485.
4. K. KAMIYA, H. HONDA, H. NASU, *Nippon Seramikkusu Kyokai Gakujutsu Ronbunshi* **98**(8) (1990) 759.
5. L. DEL OLMO and M. L. CALZADA, *J. Non-Cryst. Solids*, **121** (1990) 424.
6. C. E. KIM, Y. I. PARK and H. W. LEE, *J. Mater. Sci. Lett.* **16** (1997) 96.
7. J. M. BOULTON, G. TEOWEE and D. R. UHLMANN, "Better Ceramics through Chemistry V" (Material Research Society, Pennsylvania, 1992) p. 517.
8. Y. I. PARK, H. W. LEE, Y. S. CHOI, J. H. LEE, S. H. KIM and C. E. KIM, *J. Kor. Ceram. Soc.* **33**(7) (1996) 755.
9. V. K. SETH and W. A. SCHULZE, *Ferroelectrics* **112** (1990) 283.
10. T. R. GURURAJA, D. CHRISTOPER, R. E. NEWNHAM and W. A. SCHULZE, *Ferroelectrics* **47** (1983) 193.
11. S. KATAYAMA and M. SEKINE, "Better Ceramics through Chemistry IV" (Material Research Society, Pennsylvania, 1990) p. 897.
12. U. SELVARAG, A. V. PRASADARAO, S. KOMARNENI and R. ROY, *Mater. Lett.* **12** (1991) 311.
13. M. TOHGE, M. TATSUMISAGO and T. MINAMI, *J. Non-Cryst. Solids* **121** (1990) 443.
14. Y. TAKAHASHI, H. HAYASHI and Y. OHYA, *Mat. Res. Soc. Symp. Proc.* **271** (1992) 401.
15. D. C. BRADLEY, R. C. MEHROTRA and D. P. GAUR, "Metal Alkoxides" (Academic Press, New York, 1978) p. 226.
16. S. SAKKA, "Sol-gel Technology for Thin Films, Fibers, Preforms, and Special shapes" (Noyes, Park Ridge, New York, 1988) p. 130.
17. G. H. HAERTLING, *J. Amer. Ceram. Soc.* **43**(12) (1964) 875.
18. K. OKAZAKI, "Ceramic Engineering for Dielectrics—Fourth Edition" (Gakken-sha Publishing Co. Ltd, Tokyo, 1992) p. 518.
19. *Idem.*, in "Ceramic Engineering for Dielectrics" (Gakken-sha Publishing, Tokyo, 1992) p. 200.
20. B. JAFFE, W. R. COOK, JR. and H. Jaffe, "Piezoelectric Ceramics" (Academic Press, New York, 1971) p. 87.
21. *Idem.*, "Piezoelectric Ceramics" (Academic Press, New York, 1971) p. 169.
22. Y. XU, "Ferroelectric Materials and Their Applications" (North-Holland, New York, 1991) p. 68.
23. M. E. LINES and M. N. GLASS, "Principles and Applications of Ferroelectrics and Related Materials" (Oxford University Press, Oxford, 1977) p. 141.
24. K. OKAZAKI, "Ceramic Engineering for Dielectrics—Fourth Edition" (Gakken-sha Publishing Co. Ltd, Tokyo, 1992) p. 527.

Received 25 January
and accepted 18 September 2000